

Radiolabeled Amino Acids for Tumor Imaging with PET: Radiosynthesis and Biological Evaluation of 2-Amino-3-[¹⁸F]fluoro-2-methylpropanoic Acid and 3-[¹⁸F]Fluoro-2-methyl-2-(methylamino)propanoic Acid

Jonathan McConathy,[†] Laurent Martarello,[†] Eugene J. Malveaux,[†] Vernon M. Camp,[†] Nicholas E. Simpson,[†] Chiab P. Simpson,[†] Geoffrey D. Bowers,[‡] Jeffrey J. Olson,[‡] and Mark M. Goodman^{*,†}

Department of Radiology and Department of Neurosurgery at Emory University Hospital, School of Medicine, 1364 Clifton Road Northeast, Atlanta, Georgia 30322

Received May 31, 2001

Novel radiopharmaceuticals, including amino acids, that target neoplasms through their altered metabolic states have shown promising results in preclinical and clinical studies. Two fluorinated analogues of α -aminoisobutyric acid, 2-amino-3-fluoro-2-methylpropanoic acid (FAMP) and 3-fluoro-2-methyl-2-(methylamino)propanoic acid (*N*-MeFAMP), have been radiolabeled with fluorine-18, characterized in amino acid uptake assays, and evaluated in vivo in normal rats and a rodent tumor model. The key steps in the syntheses of both radiotracers involved the preparation of cyclic sulfamidate precursors. Radiosyntheses of both [¹⁸F]FAMP and [¹⁸F]*N*-MeFAMP via no-carrier-added nucleophilic substitution provided high yields (> 78% decay-corrected) in high radiochemical purity (> 99%). Amino acid transport assays using 9L gliosarcoma cells demonstrated that both compounds are substrates for the A type amino acid transport system, with [¹⁸F]*N*-MeFAMP showing higher specificity than [¹⁸F]FAMP for A type transport. Tissue distribution studies in normal Fischer rats and Fischer rats implanted intracranially with 9L gliosarcoma tumor cells were also performed. At 60 min postinjection, the tumor vs normal brain ratio of radioactivity was 36:1 in animals receiving [¹⁸F]FAMP and 104:1 in animals receiving [¹⁸F]*N*-MeFAMP. On the basis of these studies, both [¹⁸F]FAMP and [¹⁸F]*N*-MeFAMP are promising imaging agents for the detection of intracranial neoplasms via positron emission tomography.

Introduction

The development of radiolabeled amino acids for use as metabolic tracers to image tumors using positron emission tomography (PET) and single photon emission computed tomography (SPECT) has been underway for two decades. Although radiolabeled amino acids have been applied to a variety of tumor types, their application to intracranial tumors has received considerable attention due to potential advantages over other imaging modalities. After surgical resection and/or radiotherapy of brain tumors, conventional imaging methods such as computed tomography (CT) and magnetic resonance imaging (MRI) do not reliably distinguish residual or recurring tumor from tissue injury due to the intervention and are not optimal for monitoring the effectiveness of treatment or detecting tumor recurrence.^{1,2} The leading PET agent for diagnosis and imaging of neoplasms, 2-[¹⁸F]fluorodeoxyglucose (FDG), also has limitations in the imaging of brain tumors. Normal brain cortical tissue shows high [¹⁸F]FDG uptake as does inflammatory tissue, which can occur after radiation or surgical therapy; these factors can complicate the interpretation of images acquired with [¹⁸F]FDG.^{3–6} A number of reports indicate that PET and SPECT imaging with radiolabeled amino acids better define tumor boundaries within normal brain than CT,

MRI, or [¹⁸F]FDG, allowing better planning of treatment.^{7,8} Additionally, some studies suggest that the degree of amino acid uptake correlates with tumor grade, which could provide important prognostic information.^{8–10}

A number of amino acids, including [¹¹C] α -aminoisobutyric acid (AIB), L-[¹¹C]methionine (Met), L-[¹⁸F]-fluoro- α -methyl tyrosine, *O*-(2-[¹⁸F]fluoroethyl) tyrosine, and *anti*-1-amino-3-[¹⁸F]fluorocyclobutyl-1-carboxylic acid (FACBC), have been successfully used for PET tumor imaging in humans.^{8,11–14} AIB is a nonmetabolized α,α -dialkyl amino acid that is actively transported into cells primarily via the A type amino acid transport system. System A amino acid transport is increased during cell growth and division and has also been shown to be upregulated in tumor cells.^{15–17} Studies of experimentally induced tumors in animals and spontaneously occurring tumors in humans have shown increased uptake of radiolabeled AIB in the tumors relative to normal tissue.^{11,18–21} The *N*-methyl analogue of AIB, *N*-MeAIB, shows even more selectivity for the A type amino acid transport system than AIB.^{22,23} *N*-MeAIB has been radiolabeled with carbon-11 and is metabolically stable in humans.²⁴

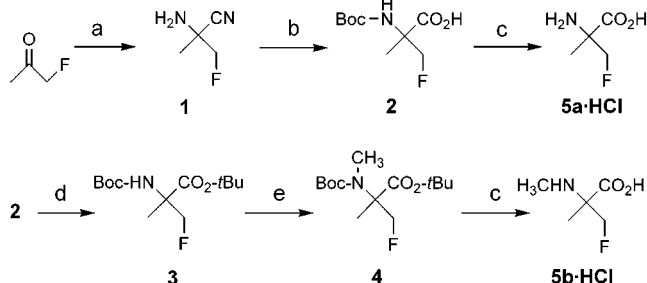
We have developed fluorinated analogues of AIB suitable for labeling with ¹⁸F and use in PET imaging. These agents are expected to demonstrate metabolic stability in vivo due to their α,α -dialkyl branching and to have the potential for remote distribution due to the 110 min half-life of ¹⁸F vs 20 min for ¹¹C. We report here the synthesis, radiolabeling, and biological evaluation

* To whom correspondence should be addressed. Tel.: (404)727-9366. Fax: (404)727-4366. E-mail: mgoodma@emory.edu.

[†] Department of Radiology.

[‡] Department of Neurosurgery.

Scheme 1. Synthesis of Fluorine-19 Amino Acids FAMP (**5a**) and *N*-MeFAMP (**5b**)^a



^a Reagents: (a) KCN, NH₄Cl, H₂O. (b) HCl and then (Boc)₂O. (c) Aqueous HCl. (d) Cl₃CC(=NH)OtBu, CH₂Cl₂. (e) NaH, DMF, CH₃I.

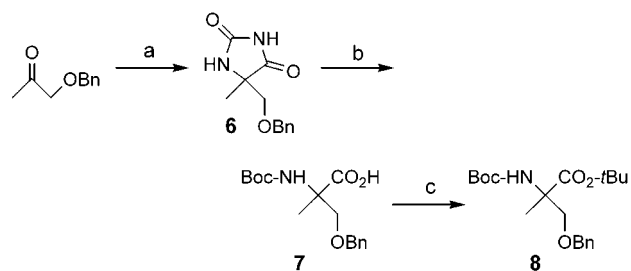
of 2-amino-3-fluoro-2-methylpropanoic acid (FAMP, **5a**) and 3-fluoro-2-methyl-2-(methylamino)propanoic acid (*N*-MeFAMP, **5b**), fluorinated analogues of AIB and *N*-methyl AIB, respectively. The dominant mechanism of cellular uptake of these radiotracers by 9L gliosarcoma cells was determined in vitro using inhibitors of amino acid transport. Tissue distribution studies in normal and 9L gliosarcoma tumor-bearing rats were carried out after intravenous administration of [¹⁸F]**5a** and [¹⁸F]**5b**, and the tumor uptake of radioactivity was compared to uptake in normal brain for both compounds.

Results and Discussion

Chemistry. The syntheses of nonradioactive **5a** and **5b** are shown in Scheme 1. For **5a**, the aminonitrile **1** was prepared from fluoroacetone using a Strecker type reaction. To facilitate purification, the carbamate **2** was prepared by treating the crude product of the acid hydrolysis of **1** with di-*tert*-butyl dicarbonate followed by flash chromatography. The amino acid **5a** was obtained as its salt in analytically pure form by treating **2** with aqueous HCl. Compound **2** could also be obtained by treating **14a** (see Scheme 4 for structure) with tetrabutylammonium fluoride and derivatizing the crude amino acid using di-*tert*-butyl dicarbonate. Preparation of **5b** was performed starting with the carbamate **2**. Treatment of **2** with *tert*-butyl-2,2,2-trichloroacetimidate under neutral conditions²⁵ provided the *N*-*tert*-butoxycarbonyl (*N*-Boc) ester **3**, which was alkylated with methyl iodide and sodium hydride in dimethylformamide (DMF) to yield **4**. Deprotection of **4** in aqueous HCl provided amino acid **5b** as its salt. Although synthesis of **5a,b** via the aminonitrile intermediate was straightforward, this strategy was not amenable to radiosynthesis of [¹⁸F]**5a** and [¹⁸F]**5b**.

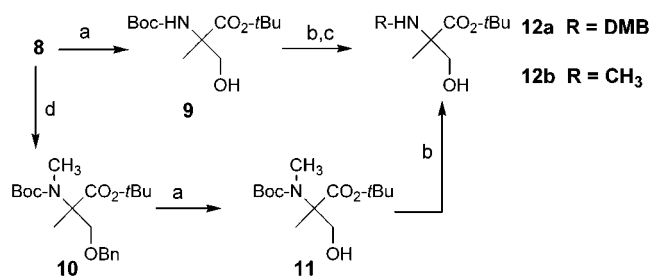
Initial attempts to prepare [¹⁸F]**5a** from a methane-sulfonyl ester precursor failed due to lack of ¹⁸F incorporation into the molecule, presumably because of the low reactivity of the β-carbon due to its neopentyl character. As an alternative, cyclic sulfamidates were attractive precursors because they have been used to prepare a number of ¹⁸F radioligands and nonradioactive α,α-disubstituted amino acid derivatives including 3-fluoro-2-(4-methoxybenzylamino)-2-methylpropanoic acid methyl ester.^{26–29} However, there are currently no literature reports of cyclic sulfamidate formation from primary amines. While this did not pose a problem

Scheme 2. Synthesis of 3-Benzyloxy-2-[*N*-(*tert*-butoxycarbonyl)amino]-2-methylpropanoic Acid *tert*-Butyl Ester (**8**)^a



^a Reagents: (a) (NH₄)₂CO₃, KCN, NH₄Cl, 1:1 EtOH:H₂O. (b) 5 N NaOH, 180 °C and then (Boc)₂O, 9:1 CH₃OH:Et₃N. (c) Cl₃CC(=NH)OtBu, CH₂Cl₂.

Scheme 3. Synthesis of *N*-Substituted Amino Alcohols **12a,b**^a



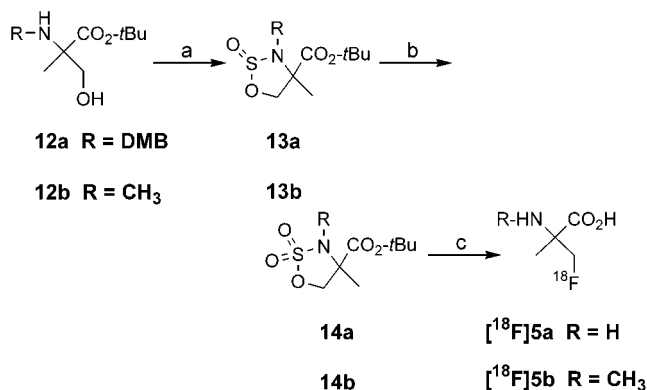
^a Reagents: (a) 10% Pd/C, H₂, CH₃OH. (b) *p*TsOH·H₂O, EtOH, 40 °C. (c) DMB-Cl, Et₃N, CH₂Cl₂. (d) NaH, DMF, CH₃I. *p*TsOH = *p*-toluenesulfonic acid, and DMB = bis(4-methoxyphenyl)methyl.

for the synthesis of [¹⁸F]**5b**, which contains a secondary amine, in the case of [¹⁸F]**5a**, it was necessary to utilize an amino substituent that was suitable for cyclic sulfamidate formation but could be readily removed during radiosynthesis (see below). For both radiotracers, the key steps in the preparation of the precursors for radiolabeling involved the synthesis of secondary amino alcohols, which could be converted to cyclic sulfamidates.

The α-methyl serine derivative **8** served as a common intermediate in the syntheses of [¹⁸F]**5a** and [¹⁸F]**5b** and was prepared as shown in Scheme 2. Treatment of 3-benzyloxypropanone with a buffered ammonium carbonate and potassium cyanide solution led to the formation of the hydantoin **6**. Alkaline hydrolysis of the hydantoin followed by treatment of the crude amino acid with di-*tert*-butyl dicarbonate gave the *N*-Boc acid **7**. The *tert*-butyl ester **8** was prepared from **7** using *tert*-butyl-2,2,2-trichloroacetimidate under neutral conditions.²⁵

The synthesis of the amino alcohols **12a** and **12b** is depicted in Scheme 3. To prepare **12a**, the alcohol **9** was obtained from the catalytic hydrogenolysis of the benzyl ether **8**. The bis(4-methoxyphenyl)methyl group, also known as 4,4'-dimethoxybenzhydryl (DMB), was incorporated because it provided a secondary amine for cyclic sulfamidate formation but could be rapidly removed under acidic conditions.³⁰ This arrangement permitted *N*-dealkylation, hydrolysis of the sulfamate obtained from nucleophilic ring opening, and hydrolysis of the *tert*-butyl ester in a single step after incorporation of ¹⁸F. Selective removal of the Boc protecting group of **9** in the presence of the *tert*-butyl ester was achieved with *p*-toluenesulfonic acid by modifying the procedure reported by Goodacre et al.³¹ While the reaction did not

Scheme 4. Synthesis of Cyclic Sulfamidates **14a,b** and Radiosynthesis of [^{18}F]FAMP (**5a**) and [^{18}F]N-MeFAMP (**5b**)^a



^a Reagents: (a) SOCl₂, Et₃N, toluene or CH₂Cl₂. (b) NaIO₄, catalytic RuO₂, H₂O, CH₃CN. (c) [^{18}F]HF, K_{2,2,2}, K₂CO₃, CH₃CN, 85 °C and then 6 N HCl, 85 °C.

proceed at 40 °C even with prolonged reaction times (>4 days), the desired intermediate was obtained rapidly when the solvent was removed under reduced pressure at 40 °C. The crude amino ester from this procedure was monoalkylated with bis(4-methoxyphenyl)chloromethane to provide **12a**.

As shown in Scheme 3, the amino alcohol **12b** was also prepared from compound **8**. First, **8** was treated with methyl iodide and sodium hydride in DMF to afford the *N*-methyl derivative **10** in quantitative yield. Catalytic hydrogenolysis of **10** provided the alcohol **11**, which was then converted to **12b** with *p*-toluenesulfonic acid as previously described.

Scheme 4 depicts the formation of the cyclic sulfamidate precursors **14a,b** and subsequent radiolabeling to produce the amino acids [^{18}F]5a and [^{18}F]5b. The amino alcohols **12a,b** were reacted with thionyl chloride in the presence of triethylamine to form cyclic sulfamidites **13a,b**. Oxidation using sodium periodate with catalytic ruthenium(IV) oxide provided **14a,b** from **13a,b**, respectively. The precursors **14a,b** are stable for at least 6 months when stored at -10 °C.

Radiochemistry. Initial attempts to synthesize [^{18}F]5a via nucleophilic substitution of the methyl sulfonyl ester of **9** did not demonstrate measurable ^{18}F incorporation after prolonged heating. In contrast, the cyclic sulfamidate precursor **14a** provided an average 78% decay-corrected yield ($n = 4$ runs) of [^{18}F]5a in over 99% radiochemical purity. Likewise, treatment of **14b** under the same conditions gave an average 85% decay-corrected yield ($n = 3$ runs) of [^{18}F]5b in over 99% radiochemical purity. The radiolabeled amino acids were prepared in a one pot synthesis by treating the precursor **14a** or **14b** with no-carrier-added [^{18}F]fluoride at 85 °C for 20 min followed by acid hydrolysis at 85 °C for 10 min. The reaction mixture was then passed through a column containing ion-retardation resin followed by alumina and C-18 SepPaks. The eluted fractions were pH 6–7 and suitable for direct use in the rodent studies. In a representative synthesis, a total of 76 mCi of [^{18}F]5b at end of synthesis (EOS) was obtained from 166 mCi of ^{18}F (end of bombardment, EOB) in a synthesis time of approximately 90 min.

While the specific activities of [^{18}F]5a and [^{18}F]5b were not determined directly, the maximum amount of

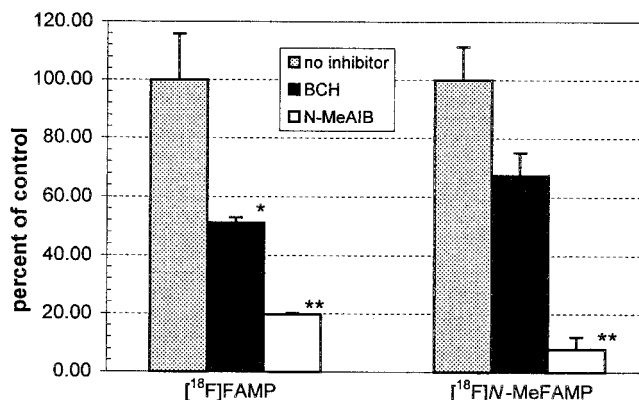


Figure 1. Inhibition of uptake of [^{18}F]FAMP (**5a**) and [^{18}F]N-MeFAMP (**5b**) by BCH and *N*-MeAIB in 9L gliosarcoma cells. Values are expressed as percent of control uptake (no inhibitor). Uptake was determined after 30 min incubations and normalized for dose and number of cells. *p*-Values represent comparisons of uptake in the presence of inhibitor to control uptake for each radiotracer (1-way ANOVA). * = $p < 0.05$, and ** = $p < 0.01$. Bars indicate standard error.

unlabeled material in the final product arising from the precursors is about 1 mg in each case. On the basis of a 100 mCi yield at the EOS, the minimum ratio of radiotracer to unlabeled material for both [^{18}F]5a and [^{18}F]5b is 1 mCi per 10 μg of unlabeled material. This amount of unlabeled material is comparable to the amount present in doses of [^{18}F]FDG, which also contain nonradioactive material arising from the triflate precursor of [^{18}F]FDG.³² In doses of [^{18}F]FDG, the majority of unlabeled material is comprised of glucose and mannose, both of which are not toxic. In the cases of [^{18}F]5a and [^{18}F]5b, the potential toxicity of the unlabeled material present in doses must be evaluated prior to the use of these compounds in human studies.

Amino Acid Uptake Assays. To test the hypothesis that [^{18}F]5a and [^{18}F]5b enter cells predominantly via the A type amino acid transport system, amino acid uptake assays using cultured 9L gliosarcoma cells in the presence and absence of two well-described inhibitors of amino acid transport were performed. *N*-MeAIB is a selective competitive inhibitor of the A type amino acid transport system while 2-amino-bicyclo[2.2.1]heptane-2-carboxylic acid (BCH) is commonly used as an inhibitor for the sodium-independent L type transport system, although this compound also competitively inhibits amino acid uptake via the sodium-dependent B^{0,+} and B⁰ transport systems.¹⁵ The A and L type amino acid transport systems have been implicated in the in vivo uptake of radiolabeled amino acids used for tumor imaging.^{8,19}

In the absence of inhibitors, both [^{18}F]5a and [^{18}F]5b showed similar levels of uptake in 9L gliosarcoma cells, with intracellular accumulations of 0.43 and 0.50% of the initial dose per million cells after 30 min of incubation, respectively. To facilitate the comparison of the effects of the inhibitors, the data were expressed as percent uptake relative to the control condition (no inhibitor) as shown in Figure 1. In the case of [^{18}F]5a, BCH blocked 48% of the uptake of activity relative to controls while *N*-MeAIB blocked 80% of uptake relative to controls. The reduction of uptake of [^{18}F]5a by both BCH and *N*-MeAIB as compared to controls was statistically significant ($p < 0.05$ and $p < 0.01$, respectively,

Table 1. Tissue Distribution of Radioactivity in Normal Fischer Rats after Injection of [¹⁸F]FAMP (**5a**)^a

tissue	5 min	30 min	60 min	120 min
blood	0.53 ± 0.03	0.25 ± 0.014	0.22 ± 0.02	0.15 ± 0.005
heart	0.29 ± 0.012	0.29 ± 0.04	0.28 ± 0.013	0.23 ± 0.03
lung	0.55 ± 0.006	0.54 ± 0.12	0.44 ± 0.05	0.37 ± 0.10
liver	0.65 ± 0.05	0.56 ± 0.04	0.50 ± 0.013	0.48 ± 0.03
spleen	0.83 ± 0.05	0.54 ± 0.03	0.50 ± 0.04	0.33 ± 0.02
pancreas	3.46 ± 0.19	2.93 ± 0.20	2.95 ± 0.27	2.48 ± 0.03
kidney	6.36 ± 0.36	5.59 ± 0.28	4.74 ± 0.15	2.97 ± 0.17
bone	0.27 ± 0.005	0.22 ± 0.02	0.19 ± 0.03	0.13 ± 0.012
muscle	0.22 ± 0.013	0.22 ± 0.009	0.26 ± 0.02	0.19 ± 0.003
testis	0.17 ± 0.010	0.10 ± 0.006	0.12 ± 0.006	0.10 ± 0.004
brain	0.04 ± 0.003	0.05 ± 0.004	0.06 ± 0.004	0.05 ± 0.001

^a Values are reported as mean percent dose per gram ± standard error. *n* = 4 at each time point.

by one way analysis of variance (ANOVA)). The magnitude of uptake inhibition of [¹⁸F]**5a** by BCH was less than that observed with *N*-MeAIB, but this difference between inhibitors did not reach statistical significance in this experiment.

In assays employing [¹⁸F]**5b**, BCH inhibited 33% of uptake of activity as compared to controls while *N*-MeAIB blocked 88% of uptake as compared to controls. Only the reduction of uptake of [¹⁸F]**5b** by *N*-MeAIB was significantly different from control uptake (*p* < 0.01 by one way ANOVA), although a trend toward reduction was observed with BCH. Also, *N*-MeAIB reduced uptake of [¹⁸F]**5b** to a greater extent than BCH (*p* < 0.05 by one way ANOVA).

Taken together, these inhibition studies indicate that [¹⁸F]**5a** and [¹⁸F]**5b** are substrates for the A type amino acid transport system in 9L gliosarcoma cells based on the inhibition of uptake of both compounds in the presence of *N*-MeAIB. Additionally, [¹⁸F]**5a** is also a substrate in vitro for at least one non-A transport system, possibly system L, based on the inhibition of uptake by BCH. The data indicate that [¹⁸F]**5b** is a more selective substrate for the A type amino transport system than [¹⁸F]**5a**, consistent with the increased selectivity of *N*-MeAIB for A type transport relative to AIB.^{22,23} Because [¹⁸F]**5a** and [¹⁸F]**5b** were evaluated as racemic mixtures, it is possible that the enantiomers of these compounds differ in their specificity for the various amino acid transport systems. A more detailed analysis of the biological transport properties of these radiotracers and their single enantiomers in a panel of other tumor cell lines is in progress.

Biodistribution in Normal Rats. The results of the biodistribution studies with [¹⁸F]**5a** in normal rats are presented in Table 1. At 5 min after tail vein injection of [¹⁸F]**5a**, both the pancreas and the kidneys showed significantly higher uptake of radioactivity than the other tissues studied (*p* < 0.001 by one way ANOVA), with 3.46 and 6.36% of the injected dose per gram of tissue (% ID/g), respectively. The activity in these tissues remained above the activity in other tissues (*p* < 0.001 by one way ANOVA at all time points), with 2.48% ID/g in the pancreas and 2.97% ID/g in the kidneys at 120 min. The liver showed moderate uptake of activity, with 0.65% ID/g at 5 min, which decreased to 0.48% ID/g after 120 min. Other tissues studied, including heart, lung, bone, blood, muscle, and testis, showed relatively low uptake of radioactivity at 5 min (<0.55% ID/g), which decreased over the course of the

Table 2. Tissue Distribution of Radioactivity in Normal Fischer Rats after Injection of [¹⁸F]*N*-MeFAMP (**5b**)^a

tissue	5 min	30 min	60 min	120 min
blood	0.61 ± 0.02	0.30 ± 0.003	0.18 ± 0.02	0.10 ± 0.007
heart	0.22 ± 0.01	0.23 ± 0.03	0.20 ± 0.02	0.17 ± 0.02
lung	0.53 ± 0.03	0.50 ± 0.07	0.38 ± 0.07	0.30 ± 0.08
liver	0.79 ± 0.06	0.72 ± 0.09	0.78 ± 0.10	0.58 ± 0.11
spleen	0.44 ± 0.06	0.75 ± 0.06	0.68 ± 0.02	0.47 ± 0.04
pancreas	2.73 ± 0.28	3.00 ± 0.23	3.24 ± 0.30	2.88 ± 0.40
kidney	8.12 ± 0.62	4.60 ± 0.70	2.73 ± 0.35	1.36 ± 0.27
bone	0.34 ± 0.04	0.32 ± 0.04	0.29 ± 0.04	0.20 ± 0.02
muscle	0.16 ± 0.008	0.16 ± 0.003	0.15 ± 0.007	0.13 ± 0.007
testis	0.17 ± 0.004	0.11 ± 0.005	0.08 ± 0.005	0.06 ± 0.005
brain	0.04 ± 0.005	0.04 ± 0.004	0.03 ± 0.003	0.03 ± 0.001

^a Values are reported as mean percent dose per gram ± standard error. *n* = 4 at each time point.

2 h study. The brain showed the lowest uptake of radioactivity, with approximately 0.05% ID/g at all time points.

The results of the biodistribution study with [¹⁸F]**5b** in normal rats were very similar to those obtained with [¹⁸F]**5a**. These results for [¹⁸F]**5b** are depicted in Table 2. The highest uptake was observed in the pancreas and the kidneys with 2.73 and 8.12% ID/g, respectively, at 5 min. As with [¹⁸F]**5a**, the brain uptake of activity was very low, with approximately 0.04% ID/g in the brain at all time points. The low brain uptake of these compounds is consistent with the observation that the A type amino transport system is not present at the intact blood–brain barrier (BBB).³³ The lack of significant accumulation of radioactivity in bone indicates that significant in vivo defluorination resulting from metabolism did not occur with either compound during the 2 h studies.

The data obtained from normal rats with both [¹⁸F]**5a** and [¹⁸F]**5b** are similar to the reported distributions of [¹¹C]AIB in rats²¹ and [¹⁴C]AIB in mice,¹⁸ suggesting that these amino acids have similar transport mechanisms in vivo. This observation is consistent with the A type transport observed for both [¹⁸F]**5a** and [¹⁸F]**5b** in vitro. In healthy Copenhagen rats, the uptake of [¹¹C]AIB at 60 min was highest in the kidneys and pancreas, with 10.3 and 6.0 mean relative concentrations (mean RC, calculated from the dose fraction in the tissue divided by tissue weight multiplied by body weight), respectively. In contrast, the brain had the lowest mean RC of [¹¹C]AIB with a value of 0.2. In nude Swiss mice bearing human melanoma transplants that received doses of [¹⁴C]AIB, similar results were obtained. The highest mean RC values were observed in the kidneys and pancreas at 60 min, with values of 3.4 and 8.6, respectively, while the brain had the lowest mean RC of organs studied with a value of 0.23. As with [¹⁸F]**5a** and [¹⁸F]**5b**, the uptake of radioactivity in the pancreas and kidneys was rapid in these studies of AIB biodistribution, with mean RC values in both tissues greater than 1.8 within 5–15 min postinjection. In both studies of AIB, moderate liver uptake of activity was observed, while the mean RC in blood and muscle was low at 60 min.

High pancreatic uptake of radioactivity has been reported for a number of other ¹¹C-labeled amino acids in rats, including Met, L-[¹¹C]leucine, and 1-aminocyclopentane-1-[¹¹C]carboxylic acid.³⁴ The pancreatic uptake ranged from approximately 3 to 5% ID/g at 60

Table 3. Tissue Distribution of Radioactivity in Tumor-Bearing Fischer Rats after Injection of [¹⁸F]FAMP (**5a**)^a

tissue	5 min	60 min	120 min
blood	0.72 ± 0.05	0.26 ± 0.03	0.16 ± 0.01
heart	0.40 ± 0.04	0.33 ± 0.06	0.22 ± 0.02
lung	0.84 ± 0.03	0.38 ± 0.04	0.24 ± 0.03
liver	0.77 ± 0.22	0.66 ± 0.16	0.25 ± 0.02
spleen	0.72 ± 0.06	0.55 ± 0.08	0.32 ± 0.02
pancreas	5.31 ± 0.68	2.86 ± 0.34	1.42 ± 0.17
kidney	8.66 ± 1.27	6.20 ± 1.45	3.64 ± 0.26
bone	0.38 ± 0.04	0.25 ± 0.05	0.16 ± 0.01
muscle	0.39 ± 0.02	0.31 ± 0.03	0.21 ± 0.01
testis	0.22 ± 0.02	0.14 ± 0.02	0.11 ± 0.003
brain	0.035 ± 0.002*	0.054 ± 0.01**	0.050 ± 0.004†
tumor	0.91 ± 0.05*	1.96 ± 0.10**	1.87 ± 0.2†
tumor:brain ratio	26:1	36:1	37:1

^a Values are reported as mean percent dose per gram ± standard error. *n* = 4 at 5 min, *n* = 5 at 60 min, and *n* = 4 at 120 min; *p* values were determined using a two-tailed *t*-test for pairwise comparisons. * = *p* < 0.001, ** = *p* < 0.001, and † = *p* < 0.003.

min in this study of these compounds. Similarly, [¹⁸F]-FACBC showed 3.4% ID/g at 60 min in normal Fischer rats. The similarity between the biodistribution patterns of [¹⁸F]**5a**, [¹⁸F]**5b**, and radiolabeled AIB, and in particular the high pancreatic and low brain uptake of radioactivity, prompted us to evaluate these compounds in tumor-bearing rats.

Biodistribution in Tumor-Bearing Rats. The tissue distribution of radioactivity after tail vein injection of [¹⁸F]**5a** in the normal tissues of tumor-bearing rats was similar to that seen in normal rats and is presented in Table 3. Tumor uptake of radioactivity at 5, 60, and 120 min after injection was 0.91, 1.96, and 1.87% ID/g, respectively, while uptake in normal brain tissue contralateral to the tumor was approximately 0.05% ID/g at each time point. The higher uptake of activity by the tumor vs normal brain was statistically significant at each time point (*p* < 0.001 at 5 and 60 min and *p* < 0.003 at 120 min by two-tailed paired *t*-tests). The resulting ratios of tumor uptake to normal brain uptake were 26:1, 36:1, and 37:1 at 5, 60, and 120 min, respectively.

The results from the same study conducted with [¹⁸F]-**5b** in tumor-bearing rats are summarized in Table 4 and demonstrated tumor uptake of 1.29, 2.28, and 1.94% ID/g at 5, 60, and 120 min postinjection, respectively. At each time point, the higher uptake of activity in the tumor vs normal brain tissue was statistically significant (*p* < 0.02 at 5 min and *p* < 0.001 at 60 and 120 min by two-tailed paired *t*-tests). The ratios of tumor uptake to normal brain uptake at 5, 60, and 120 min obtained with [¹⁸F]**5b** were 40:1, 104:1, and 97:1, respectively. Because of the relatively long intervals between time points, it is possible that the highest tumor to brain ratio was not observed for [¹⁸F]**5a** or [¹⁸F]-**5b**. Imaging studies in nonhuman primates and in human cancer patients will provide more detailed information regarding the biodistribution and kinetics of tracer uptake in normal and neoplastic tissue.

For both [¹⁸F]**5a** and [¹⁸F]**5b**, the ratios of tumor to brain uptake of activity are higher than those reported for [¹⁸F]FDG and [¹⁸F]FACBC in the same rodent tumor model.¹⁴ In the case of [¹⁸F]FDG, the tumor to brain ratio was 0.8:1 at 60 min with 1.30% ID/g in normal

Table 4. Tissue Distribution of Radioactivity in Tumor-Bearing Fischer Rats after Injection of [¹⁸F]N-MeFAMP (**5b**)^a

tissue	5 min	60 min	120 min
blood	0.69 ± 0.04	0.17 ± 0.02	0.10 ± 0.007
heart	0.34 ± 0.02	0.25 ± 0.03	0.19 ± 0.02
lung	0.61 ± 0.04	0.26 ± 0.03	0.19 ± 0.011
liver	0.94 ± 0.12	0.85 ± 0.17	0.41 ± 0.06
spleen	0.47 ± 0.04	0.45 ± 0.06	0.40 ± 0.02
pancreas	2.95 ± 0.58	2.42 ± 0.27	1.74 ± 0.24
kidney	9.33 ± 0.36	2.79 ± 0.31	1.59 ± 0.19
bone	0.33 ± 0.04	0.23 ± 0.04	0.19 ± 0.02
muscle	0.22 ± 0.011	0.19 ± 0.02	0.16 ± 0.012
testis	0.19 ± 0.008	0.08 ± 0.008	0.08 ± 0.005
brain	0.032 ± 0.002*	0.022 ± 0.006**	0.020 ± 0.005†
tumor	1.29 ± 0.28*	2.28 ± 0.16**	1.94 ± 0.12†
tumor:brain ratio	40:1	104:1	97:1

^a Values are reported as mean percent dose per gram ± standard error. *n* = 4 at each time point; *p* values were determined using a two-tailed *t*-test for pairwise comparisons. * = *p* < 0.02, ** = *p* < 0.001, and † = *p* < 0.001.

brain and 1.05% ID/g in the tumor tissue, demonstrating the high levels of [¹⁸F]FDG uptake in normal brain tissue. At 60 min postinjection, [¹⁸F]FACBC showed a 7:1 tumor to brain ratio with 1.72% ID/g in tumor tissue vs 0.26% ID/g in normal brain. A similar ratio of tumor to brain uptake of radiotracer was seen with [¹⁸F]-FACBC in a PET scan of a human volunteer with biopsy-confirmed glioblastoma multiforme (6:1 ratio at 20 min postinjection), suggesting that this rodent model is useful in predicting imaging properties of radiolabeled amino acids in human patients with brain tumors.

As in the normal rats receiving [¹⁸F]**5a** or [¹⁸F]**5b**, high levels of uptake occurred in the pancreas and kidneys of the tumor-bearing rats. Additionally, both compounds had high uptake in tumor tissue but relatively low uptake in other tissues examined including heart, lung, muscle, liver, bone, and testis. Interestingly, [¹⁸F]FACBC showed lower uptake in the kidneys in the same animal model (0.60% ID/g at 60 min), which may reflect less reuptake from the glomerular filtrate but higher uptake in the liver (1.70% ID/g at 60 min).¹⁴ On the basis of the rodent data, the pancreas, kidneys, and bladder would be predicted to bear the highest dosimetry burden in human studies employing [¹⁸F]**5a** or [¹⁸F]-**5b**. The low uptake in other normal tissues suggests that both [¹⁸F]**5a** and [¹⁸F]**5b** might be suitable for imaging tumors exhibiting high uptake of these amino acids in locations other than the brain. For example, the tumor to muscle ratios obtained at 60 min were 6.3:1 for [¹⁸F]**5a** and 12:1 for [¹⁸F]**5b**, while ratios of 5.3:1 for [¹⁸F]FDG and 4.2:1 for [¹⁸F]FACBC were observed at this time point.¹⁴ Because both [¹⁸F]**5a** and [¹⁸F]**5b** were evaluated as racemic mixtures, it is possible that the single enantiomers of [¹⁸F]**5a** and [¹⁸F]**5b** would exhibit different biodistribution profiles. If one enantiomer has superior in vivo properties for tumor imaging, using it would be advantageous in terms of both radiation dosimetry and interpretation of tissue uptake of radioactivity. The isolation and evaluation of the *R* and *S* enantiomers of both [¹⁸F]**5a** and [¹⁸F]**5b** are underway.

A comparison of the uptake of radioactivity in tumor tissue and brain tissue after [¹⁸F]**5a** and [¹⁸F]**5b** administration is depicted in Figure 2a,b. The higher ratios of tumor to brain uptake obtained with [¹⁸F]**5b** vs [¹⁸F]**5a** appear to be due to lower brain uptake of

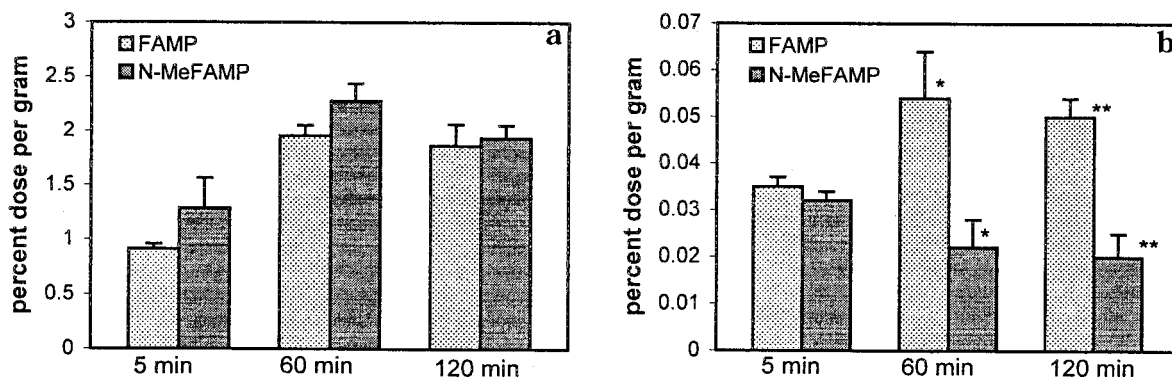


Figure 2. (a) Comparison of activity in tumor tissue after injection of [^{18}F]FAMP (**5a**) and [^{18}F]N-MeFAMP (**5b**). Tissues were compared at each time point by two-tailed *t*-test. No significant differences were detected. Bars indicate standard error. (b) Comparison of activity in normal brain after injection of [^{18}F]FAMP (**5a**) and [^{18}F]N-MeFAMP (**5b**). Tissues were compared at each time point by two-tailed *t*-test. * = $p < 0.03$, and ** = $p < 0.003$. Bars indicate standard error.

activity with [^{18}F]**5b** rather than higher tumor uptake of activity. No statistically significant differences were detected between the two compounds when comparing the uptake of activity in the tumor at the three time points studied (see Figure 2a). This observation is consistent with the amino acid uptake assay in which cultured 9L gliosarcoma cells accumulated [^{18}F]**5a** and [^{18}F]**5b** in similar amounts. However, at both 60 and 120 min postinjection, the uptake of radioactivity in the normal brain tissue of rats receiving [^{18}F]**5b** was significantly less than in animals receiving [^{18}F]**5a**. At 60 min after [^{18}F]**5a** injection, the brain uptake was 0.054 vs 0.022% ID/g in animals receiving [^{18}F]**5b** ($p < 0.03$ by a two-tailed *t*-test); at 120 min after [^{18}F]**5a** injection, the brain uptake was 0.050 vs 0.020% ID/g in animals receiving [^{18}F]**5b** ($p < 0.003$ by a two-tailed *t*-test). The magnitude of the difference in brain uptake between the compounds is enough to account for the difference in tumor to brain uptake ratios at these time points.

It is likely that the difference in normal brain uptake of activity is due to the higher selectivity of [^{18}F]**5b** vs [^{18}F]**5a** for the A type amino acid transport system, which is not active at the normal BBB.³³ Some of the other amino acid transport systems, such as the L type transport system, are active at the normal BBB¹⁹ and could potentially mediate uptake of these radiolabeled amino acids. The A type amino acid transport system tolerates amino acid substrates with an *N*-methyl group while the other amino acid transport systems generally do not,^{15,22,23} and the uptake inhibition assays discussed earlier suggest that [^{18}F]**5b** is a more selective substrate for A type transport than [^{18}F]**5a**. The lower uptake of activity observed with [^{18}F]**5b** relative to [^{18}F]**5a** in normal brain but not in tumor or pancreatic tissue is consistent with the increased selectivity of *N*-methyl amino acids for the A type amino acid transport system. If [^{18}F]**5a** and [^{18}F]**5b** were entering normal brain by diffusion alone, the more lipophilic [^{18}F]**5b** would be expected to show higher brain uptake than [^{18}F]**5a**.

The high uptake of [^{18}F]**5a** and [^{18}F]**5b** in tumor tissue combined with low uptake in normal brain accounts for the high tumor to brain ratios observed with these compounds, but the low uptake across the normal BBB may also present difficulties in PET imaging studies of brain tumors. Disruptions of the BBB due to nonneoplastic processes may lead to increased uptake of

radioactivity in lesions relative to normal brain tissue. Conversely, low grade neoplasms may have normal BBBs that do not permit these radiotracers to reach the tumor cells. These potential problems must be addressed as the compounds undergo further evaluation. However, subtle alterations in BBB metabolism and transport may precede gross disruption of the BBB in low grade tumors, and tumors outside the central nervous system would not be liable to this effect.

Conclusions. The work presented here demonstrates that both [^{18}F]**5a** and [^{18}F]**5b** can be produced in high radiochemical yield (>78% EOB) and high radiochemical purity from stable precursors and are potentially valuable agents for imaging brain tumors with PET. The synthetic strategy developed for [^{18}F]**5a** provides an efficient route for preparing radiolabeled primary amines with ^{18}F in the β position. Uptake inhibition studies using 9L gliosarcoma cells demonstrated that both compounds are substrates for the A type amino acid transport system, and these compounds represent the first report of ^{18}F -labeled amino acids that undergo significant uptake via A type transport. Biodistribution studies with both compounds showed rapid and persistent accumulation of radioactivity in rodent brain tumors with an excellent signal to background ratio. Injection of [^{18}F]**5b** led to ratios of 104:1 and 97:1 in tumor vs normal brain at 60 and 120 min, respectively, while injection of [^{18}F]**5a** led to ratios of 36:1 and 37:1 at the same time points. With the exception of the pancreas and kidneys, other tissues studied including muscle, lung, heart, and liver showed relatively low uptake of radioactivity. Studies are currently underway to determine the toxicity, metabolic stability, and radiation dosimetry associated with [^{18}F]**5a** and [^{18}F]**5b** administration and to determine the transport properties of the isolated *R* and *S* enantiomers of these compounds.

Experimental Section

Chemistry. All reagents used were obtained from commercially available sources. Solvents used in reactions were purchased from Aldrich Chemicals while solvents for chromatography were obtained from VWR. Melting points are uncorrected and were determined in capillary tubes on an Electrochemical 9100 apparatus. ^1H nuclear magnetic resonance (NMR) spectra were recorded on a Varian spectrometer at 400 MHz unless otherwise indicated and referenced to the NMR solvent (chemical shifts in δ values, *J* in Hz). Mass spectra

were determined on a VG 70-S double-focusing mass spectrometer using high-resolution electron ionization. Elemental analyses were performed by Atlantic Microlabs, Inc. and were within $\pm 0.4\%$ unless otherwise stated. The phrase "usual work up" refers to the use of anhydrous magnesium sulfate followed by concentration under reduced pressure. The compounds 3-benzoyloxypropanone³⁵ and bis(4-methoxyphenyl)chloromethane³⁶ were prepared according to literature procedures. The target compounds **5a,b** were prepared as racemic mixtures in both their fluorine-18 and fluorine-19 forms.

2-Amino-2-cyano-3-fluoropropane (1). To a solution of 1 equiv of NH_4Cl (700 mg) and 1 equiv of KCN (853 mg) in 10 mL of H_2O was added fluoroacetone (1.0 g, 13.1 mmol) in 3 mL of H_2O . After it was stirred overnight at room temperature, the reaction mixture was basified with 10 mL of 1 N NaOH and extracted with 5×20 mL of Et_2O . Usual work up afforded the aminonitrile **1** as a clear oil (510 mg, 38%), which was used without further purification. $^1\text{H NMR}$ (CDCl_3), 300 MHz: δ 1.48 (3H, d, $J = 2.1$), 4.17–4.33 (1H, m), 4.33–4.49 (1H, m).

2-[N-(tert-Butoxycarbonyl)amino]-3-fluoro-2-methylpropanoic Acid (2). The crude aminonitrile **1** (510 mg, 5.00 mmol) was refluxed overnight in 20 mL of 6 N HCl, and the solvent was removed under reduced pressure. The crude white solid was dissolved in 20 mL of 85:15 $\text{CH}_3\text{OH}:\text{Et}_3\text{N}$ and treated with 2.6 equiv of di-*tert*-butyl dicarbonate (2.8 g). After the mixture was stirred overnight, the solvent was removed under reduced pressure, and the resulting paste was stirred in ice-cold 1:1 EtOAc:0.2 N aqueous HCl for 5 min. The aqueous layer was further extracted with 2×50 mL of ice-cold EtOAc. The combined organic layers were washed with 2×50 mL of H_2O followed by usual work up. Purification by silica gel column chromatography (10% CH_3OH in CH_2Cl_2) provided **2** (767 mg, 69%) as a light yellow solid suitable for use in the next step. Analytically pure samples were obtained using the same procedure followed by further purification by silica gel column chromatography (1:3 EtOAc:hexane followed by 1:1 EtOAc:hexane) to provide the *N*-Boc acid **2** as a white solid; mp 122–123 °C (EtOAc/hexane). $^1\text{H NMR}$ (CDCl_3): δ 1.45 (9H, s), 1.56 (3H, d, $J = 1.6$), 4.74 (2H, d, $J = 46.8$), 5.30 (1H, broad s). Anal. ($\text{C}_9\text{H}_{16}\text{FNO}_4$) C, H, N.

2-[N-(tert-Butoxycarbonyl)amino]-3-fluoro-2-methylpropanoic Acid tert-Butyl Ester (3). The *N*-Boc acid **2** (767 mg, 3.46 mmol) in 10 mL of dry CH_2Cl_2 was stirred overnight with 3 equiv of *tert*-butyl-2,2,2-trichloroacetimidate (2.27 g). After it was concentrated under reduced pressure, the crude product was purified by silica gel column chromatography (5% EtOAc in hexane) to provide **3** (510 mg, 53%) as a white solid; mp 41–42 °C (EtOAc/hexane). $^1\text{H NMR}$ (CDCl_3): δ 1.44 (9H, s), 1.47 (3H, d, $J = 2.4$), 1.48 (9H, s), 4.57–4.85 (2H, m), 5.34 (1H, broad s). Anal. ($\text{C}_{13}\text{H}_{24}\text{FNO}_4$) C, H, N.

2-[N-(tert-Butoxycarbonyl)methylamino]-3-fluoro-2-methylpropanoic Acid tert-Butyl Ester (4). To a solution of **3** (200 mg, 0.72 mmol) in dry DMF under an argon atmosphere was added 8 equiv of CH_3I (0.36 mL) followed by 2 equiv of 95% NaH (37 mg). The reaction mixture was stirred overnight at room temperature. The reaction mix was added to 15 mL of H_2O and extracted with 3×15 mL of Et_2O . The combined organic layers were washed with 3×20 mL H_2O followed by the usual work up. Purification of the crude product via silica gel column chromatography (7.5% EtOAc in hexane) afforded the methylated species **4** (181 mg, 86%) as a colorless oil. $^1\text{H NMR}$ (CDCl_3): δ 1.44 (9H, s), 1.46 (9H, s), 1.51 (3H, s), 2.94 (3H, s), 4.51–5.04 (2H, m). Anal. ($\text{C}_{14}\text{H}_{26}\text{FNO}_4$) C, H, N.

FAMP (5a), Hydrochloride Salt. The *N*-Boc amino acid **2** (30 mg, 0.14 mmol) was suspended in 0.3 mL of 4 N HCl and heated to 50 °C for 90 min. The resulting homogeneous solution was evaporated under reduced pressure to provide the crude HCl salt of the amino acid. The solid was washed with 2×10 mL of Et_2O to provide **5a** (18 mg, 84%) as a white solid; decomp 204–206 °C. $^1\text{H NMR}$ (D_2O): δ 1.52 (3H, s), 4.55–4.91 (2H, m). Anal. ($\text{C}_4\text{H}_9\text{ClFNO}_2$) C, H, N.

N-MeFAMP (5b), Hydrochloride Salt. The *N*-Boc *tert*-butyl ester **4** (30 mg, 0.10 mmol) was stirred in 0.6 mL of 6 N

HCl and heated to 70 °C for 3 h. The resulting solution was evaporated under reduced pressure, and the solid was washed with 2×10 mL of Et_2O to provide **5b** (16 mg, 91%) as a white solid; decomp 178–181 °C. $^1\text{H NMR}$ (D_2O): δ 1.47–1.48 (3H, m), 2.73 (3H, s), 4.64–4.90 (2H, m). Anal. ($\text{C}_5\text{H}_{11}\text{ClFNO}_2$) C, H, N.

1-Methyl-1-(benzyloxymethyl)hydantoin (6). To a solution of 3-benzoyloxypropanone (5.7 g, 34.7 mmol) in 180 mL of 1:1 EtOH: H_2O was added 10 equiv of ammonium carbonate (33 g) followed by 4 equiv of ammonium chloride (7.42 g). After the mixture was stirred at room temperature for 30 min, a 4.5 equiv portion of potassium cyanide (10.2 g) was added, and the reaction mix was stirred for 48 h at room temperature. The solvent was evaporated under reduced pressure, and the resulting solid was washed with 3×30 mL of water to afford the hydantoin **6** (6.4 g, 79% yield) as a yellowish solid suitable for use in the next step. Analytically pure samples were obtained via chromatography on silica gel (EtOAc); mp 94.5–96 °C (EtOAc). $^1\text{H NMR}$ (CDCl_3): δ 1.43 (3H, s), 3.47 (1H, d, $J = 9.6$), 3.62 (1H, d, $J = 9.6$), 4.50–4.60 (2H, m), 5.37 (1H, broad s), 7.27–7.38 (5H, m) 7.45 (1H, broad s). Anal. ($\text{C}_{12}\text{H}_{14}\text{N}_2\text{O}_3$) C, H, N.

3-Benzoyloxy-2-[N-(tert-butoxycarbonyl)amino]-2-methylpropanoic Acid (7). A suspension of the hydantoin **6** (2.0 g, 8.5 mmol) in 55 mL of 5 M NaOH was heated at 180 °C overnight in a sealed steel vessel. After it was cooled, the reaction mix was brought to pH 7 using concentrated HCl, and the solvent was evaporated under reduced pressure. The white solid was extracted with 4×20 mL of hot EtOH, and the combined extracts were concentrated under reduced pressure. The resulting residue was dissolved in 50 mL of 9:1 $\text{CH}_3\text{OH}:\text{Et}_3\text{N}$ and treated with 2 equiv of di-*tert*-butyl dicarbonate (3.72 g) overnight at room temperature. The reaction mixture was concentrated under reduced pressure and purified by silica gel column chromatography (5% CH_3OH in CH_2Cl_2) to afford **7** as an off-white solid (1.76 g, 67%); mp 112.5–114.5 °C ($\text{CH}_3\text{OH}/\text{CH}_2\text{Cl}_2$). $^1\text{H NMR}$ (CDCl_3): δ 1.45 (9H, s), 1.46 (3H, s), 3.72 (1H, d, $J = 9.2$), 3.81 (1H, d, $J = 9.6$), 4.59 (2H, d, $J = 1.6$), 5.44 (1H, broad s), 7.30–7.38 (5H, m). Anal. ($\text{C}_{16}\text{H}_{23}\text{NO}_5$) C, H, N.

3-Benzoyloxy-2-[N-(tert-butoxycarbonyl)amino]-2-methylpropanoic Acid tert-Butyl Ester (8). To a solution of the *N*-Boc carboxylic acid **7** (1.6 g, 5.17 mmol) in 15 mL of CH_2Cl_2 at room temperature was added a 3 equiv portion of *tert*-butyl-2,2,2-trichloroacetimidate (3.4 g). After it was stirred overnight at room temperature, the solvent was evaporated under reduced pressure. Purification via silica gel column chromatography (15% EtOAc in hexane) afforded **8** as a colorless oil (1.71 g, 90%). $^1\text{H NMR}$ (CDCl_3): δ 1.44 (9H, s), 1.45 (9H, s), 1.48 (3H, s), 3.66 (1H, d, $J = 8.8$), 3.79–3.82 (1H, broad d), 4.48–4.58 (2H, m), 5.51 (1H, broad s), 7.28–7.35 (5H, m). Anal. ($\text{C}_{20}\text{H}_{31}\text{NO}_5$) C, H, N.

2-[N-(tert-Butoxycarbonyl)amino]-3-hydroxy-2-methylpropanoic Acid tert-Butyl Ester (9). A suspension of the benzyl ether **8** (540 mg, 1.48 mmol) and 10% Pd–C (130 mg) in 20 mL of CH_3OH was stirred under an H_2 atmosphere overnight. The reaction mixture was filtered over Celite, and the filtrate was concentrated under reduced pressure. Purification via silica gel column chromatography (30% EtOAc in hexane) provided a quantitative yield of **9** (407 mg, 100%) as a colorless solid; mp 44–45 °C (EtOAc/hexane). $^1\text{H NMR}$ (CDCl_3): δ 1.437 (3H, s), 1.442 (9H, s), 1.48 (9H, s), 3.72 (1H, d, $J = 11.2$), 4.00 (1H, d, $J = 11.2$), 5.32 (1H, broad s). Anal. ($\text{C}_{13}\text{H}_{25}\text{NO}_5$) C, H, N.

3-Benzoyloxy-2-[N-(tert-butoxycarbonyl)methylamino]-2-methylpropanoic Acid tert-Butyl Ester (10). The same procedure used to obtain **4** was employed using 745 mg of **8** (2.04 mmol). The crude product was purified via silica gel column chromatography (10% EtOAc in hexane) to provide **10** (770 mg, 99%) as a colorless oil. $^1\text{H NMR}$ (CDCl_3): δ 1.43 (18H, s), 1.50 (3H, s), 2.96 (3H, s), 3.67 (1H, d, $J = 10$), 4.04 (1H, broad s), 4.52 (2H, s), 7.24–7.34 (5H, m). Anal. ($\text{C}_{21}\text{H}_{33}\text{NO}_5$) C, H, N.

2-[N-(tert-Butoxycarbonyl)methylamino]-3-hydroxy-2-methylpropanoic Acid tert-Butyl Ester (11). The same hydrogenolysis conditions used to convert **8** to **9** were applied to a 350 mg portion of **10** (0.92 mmol) to afford **11** (266 mg, 100%) as a colorless oil. ¹H NMR (CDCl₃): δ 1.45–1.46 (21H, m), 2.88 (3H, s), 3.50 (1H, d, *J* = 14.8 Hz), 4.02 (1H, *J* = 15.6 Hz). Anal. (C₁₄H₂₇NO₅) C, H, N.

3-Hydroxy-2-(N[bis(4-methoxyphenyl)methyl]amino)-2-methylpropanoic Acid tert-Butyl Ester (12a). To a solution of the alcohol **9** (100 mg, 0.36 mmol) in 2 mL of diethyl ether was added 1 equiv of *p*-toluenesulfonic acid monohydrate (69 mg) dissolved in 6 mL of EtOH. The reaction mixture was concentrated under reduced pressure at 40 °C, and the residue was dissolved in 6 mL of EtOH and concentrated again. This process was repeated four times, at which time no starting material was present on thin-layer chromatography (TLC) analysis. The resulting white solid was suspended in 3 mL of CH₂Cl₂ and treated with 4.5 equiv of triethylamine (0.23 mL) followed by 1 equiv of bis(4-methoxyphenyl)chloromethane (95 mg). The reaction mixture was stirred for 1 h at room temperature. The solution was then partitioned between 10 mL of EtOAc and 10 mL of H₂O. The aqueous layer was extracted with 10 mL of EtOAc followed by the usual work up of the combined organic layers. Purification by silica gel column chromatography (20% EtOAc in hexane) provided the amino ester **12a** as a colorless oil (107 mg, 73% from **9**). ¹H NMR (CDCl₃): δ 1.17 (3H, s), 1.46 (9H, s), 3.35 (1H, d, *J* = 11.2), 3.44 (1H, d, *J* = 11.2), 3.76 (3H, s), 3.77 (3H, s), 4.82 (1H, s), 6.80–6.84 (4H, m), 7.27–7.31 (4H, m). Anal. (C₂₃H₃₁NO₅) C, H, N.

3-Hydroxy-2-methyl-2-(methylamino)propanoic Acid tert-Butyl Ester (12b). A 255 mg portion of alcohol **11** (0.88 mmol) was treated with 1 equiv *p*-toluenesulfonic acid (167 mg) as described in the preparation of **12a**. The resulting solid was added to 15 mL of 10% Na₂CO₃ and extracted with 3 × 15 mL of EtOAc. The combined organic layers were subject to the usual work up. Purification via silica gel column chromatography (10% CH₃OH in CH₂Cl₂) afforded **12b** (115 mg, 69%) as a colorless oil. ¹H NMR (CDCl₃): δ 1.24 (3H, s), 1.48 (9H, s), 2.32 (3H, s), 3.52 (1H, d, *J* = 10.8), 3.64 (1H, d, *J* = 10.8). HRMS calcd for C₉H₁₉NO₃, 189.13649; found, 189.13627. Anal. (C₉H₁₉NO₃) Calcd: C, 57.12; H, 10.12; N, 7.40. Found: C, 55.87; H, 10.05; N, 7.18.

3-[Bis(4-methoxyphenyl)methyl]-4-methyl-1,2,3-oxathiazolidine-4-carboxylic Acid tert-Butyl Ester 2-Oxide (13a). A solution of the amino alcohol **12a** (105 mg, 0.26 mmol) and 2.2 equiv of triethylamine (80 μL) in 8 mL of toluene under an argon atmosphere was cooled in an ice bath followed by the dropwise addition of 1.1 equiv of thionyl chloride (34 mg) in 1 mL of toluene. After 15 min, the ice bath was removed, and the reaction was continued for 10 min. The reaction mix was partitioned between 10 mL of EtOAc and 10 mL of H₂O. The aqueous layer was further extracted with 3 × 10 mL of EtOAc. The organic layers were combined and washed with 20 mL of brine followed by usual work up. Silica gel column chromatography (25% EtOAc in hexane) afforded a 1.6:1 mixture of cyclic sulfamidate diastereomers **13a** as a colorless oil (97 mg, 83%). ¹H NMR (CDCl₃) for major diastereomer: δ 1.32 (9H, s), 1.37 (3H, s), 3.78 (3H, s), 3.79 (3H, s), 4.23 (1H, d, *J* = 8.4), 5.34 (1H, d, *J* = 8.8), 5.91 (1H, s), 6.83–6.86 (4H, m), 7.17–7.20 (2H, m), 7.38–7.41 (2H, m). ¹H NMR (CDCl₃) for minor diastereomer: δ 1.21 (3H, s), 1.53 (9H, s), 3.77 (3H, s), 3.81 (3H, s), 4.67 (2H, s), 5.74 (1H, s), 6.82–6.91 (4H, m), 7.33–7.36 (2H, m), 7.51–7.54 (2H, m). Anal. for mixture of diastereomers: (C₂₃H₂₉NO₆S) C, H, N.

3,4-Dimethyl-1,2,3-oxathiazolidine-4-carboxylic Acid tert-Butyl Ester 2-Oxide (13b). A solution containing a 103 mg portion of **12b** (0.55 mmol) and a 2.2 equiv portion of triethylamine (0.17 mL) in 2 mL of CH₂Cl₂ was added dropwise to a solution of 1.1 equiv thionyl chloride (72 mg) in 2 mL of dry CH₂Cl₂ under argon at –78 °C. The reaction mix was allowed to warm to room temperature overnight. The reaction mix was partitioned between 10 mL of EtOAc and 10 mL of H₂O. The aqueous layer was further extracted with 2 × 10

mL of EtOAc. The organic layers were combined and washed with 20 mL of brine followed by usual work up. Purification by silica gel column chromatography (15% EtOAc in hexane) provided a 1.8:1 mixture of diastereomers **13b** (76 mg, 58%) as a colorless oil. The mixture of diastereomers was used immediately in the next step as the compounds decomposed over time. The diastereomers could be separated in small amounts using the same chromatography conditions. ¹H NMR (CDCl₃) for major diastereomer: δ 1.47 (9H, s), 1.56 (3H, s), 2.86 (3H, s), 4.55 (1H, d, *J* = 9.2), 4.73 (1H, d, *J* = 8.8). Anal. (C₉H₁₇NO₄S) Calcd: C, 45.94; H, 7.28; N, 5.95. Found: C, 45.10; H, 7.59; N, 5.64. ¹H NMR (CDCl₃) for minor diastereomer: δ 1.44 (3H, s), 1.49 (9H, s), 2.91 (3H, s), 4.03 (1H, d, *J* = 8.0), 5.22 (1H, d, *J* = 8.4). Anal. (C₉H₁₇NO₄S) Calcd: C, 45.94; H, 7.28; N, 5.95. Found: C, 46.48; H, 7.41; N, 5.78.

3-[Bis(4-methoxyphenyl)methyl]-4-methyl-1,2,3-oxathiazolidine-4-carboxylic Acid tert-Butyl Ester 2,2-Dioxide (14a). A solution of the diastereomeric sulfamidites **13a** (97 mg, 0.22 mmol) in 4 mL of CH₃CN was cooled in an ice bath and treated successively with 1.1 equiv of NaIO₄ (51 mg), a catalytic amount of RuO₂·H₂O (~1 mg), and 2.4 mL of H₂O. After 5 min of stirring, the ice bath was removed, and the reaction was continued for 20 min. The reaction mixture was diluted in 10 mL of EtOAc and washed with 10 mL of saturated NaHCO₃ solution. The aqueous layer was extracted with 2 × 10 mL of EtOAc, and the combined organic layers were washed with 10 mL of brine followed by usual work up. The crude product was purified by silica gel column chromatography (30% EtOAc in hexane) to provide the cyclic sulfamidate **14a** as a light yellow solid (90 mg, 89%); mp 143.5–145 °C (EtOAc/hexane). ¹H NMR (CDCl₃): δ 1.29 (3H, s), 1.51 (9H, s), 3.77 (3H, s), 3.80 (3H, s), 4.16 (1H, d, *J* = 8.8), 4.73 (1H, d, *J* = 8.8), 5.98 (1H, s), 6.82–6.89 (4H, m), 7.38–7.44 (4H). Anal. (C₂₃H₂₉NO₇S) C, H, N.

3,4-Dimethyl-1,2,3-oxathiazolidine-4-carboxylic Acid tert-Butyl Ester 2,2-Dioxide (14b). The same reaction conditions used to obtain **14a** were applied to 42 mg of **13b** (0.18 mmol), providing **14b** (42 mg, 94%) as a white solid; mp 54–55 °C (EtOAc/hexane). ¹H NMR (CDCl₃): δ 1.50 (9H, s), 1.52 (3H, s), 2.93 (3H, s), 4.22 (1H, d, *J* = 8.8), 4.88 (1H, d, *J* = 8.8). Anal. (C₉H₁₇NO₅S) C, H, N.

Preparation of 5a (FAMP) Via 14a. To a solution of the cyclic sulfamidate **14a** (130 mg, 0.28 mmol) in CH₃CN (4 mL) was added 3 equiv of tetrabutylammonium fluoride (1.0 M in tetrahydrofuran (THF)), and the resulting solution was stirred overnight at room temperature. The reaction mix was concentrated under reduced pressure, and the residue was treated with 5 mL of 3 N HCl at 85 °C for 1 h. After the mixture was cooled, the aqueous solution was washed with 5 mL of ether and then brought to pH 7 with 6 N NaOH. The solvent was removed under reduced pressure, and the resulting white solid was dissolved in 9:1 CH₃OH:Et₃N. To this solution was added a 2 equiv portion of (Boc)₂O (122 mg), and the reaction mixture was stirred overnight at room temperature. The work up and purification were performed as previously described to provide the product **5a** (25 mg, 40%), which had the same ¹H NMR spectrum as the product obtained via the aminonitrile route.

Radiosynthesis of [¹⁸F]5a (FAMP) and [¹⁸F]5b (N-MeFAMP). The same conditions were used to prepare [¹⁸F]-**5a** from **14a** and [¹⁸F]-**5b** from **14b**. To a Wheaton vial containing 150–200 mCi of no-carrier-added [¹⁸F]HF (20 μA, 10–15 min bombardment, theoretical specific activity of 1.7 Ci/nmole) in 350 μL of [¹⁸O]H₂O were added a 1 mL solution of 10 mg K₂222 Kryptofix and 1 mg of K₂CO₃ in CH₃CN. The solvent was removed at 115 °C with argon gas flow, and an additional 1 mL of CH₃CN was added followed by evaporation with argon flow. This drying was repeated a total of three times to remove residual H₂O. A 1–2 mg portion of the cyclic sulfamidate precursor **14a,b** in 1 mL of dry CH₃CN was added to the vial, and the reaction mix was heated at 85 °C for 20 min. The solvent was removed at 115 °C with argon gas flow, and the intermediate product was treated with 0.5 mL of 6 N HCl at 85 °C for 10 min. The solution of radiolabeled amino acid was diluted in 1–2 mL of H₂O and eluted in H₂O through

a 7 mm × 120 mm column of ion-retardation resin (Bio Rad AG11A8 50–100 mesh) in series with 2 Alumina N SepPaks and 1 C-18 SepPak. The eluting fractions containing radioactivity were used directly in rodent studies. The identity of the radiolabeled product was confirmed by comparing the R_f of the radioactive product visualized with radiometric TLC with the R_f of the authentic ^{18}F compound visualized with ninhydrin stain ($R_f = 0.6$, Alltech 0.25 mm RP Chiralplates, 20:5:5 $\text{CH}_3\text{CN}:\text{H}_2\text{O}:\text{MeOH}$). In all radiosyntheses, the only peak present on radiometric TLC analysis corresponded to **5a,b**, and the radiochemical purity of the product exceeded 99%. The isolated radiochemical yields were determined using a dose calibrator (Capintec CRC-712M).

Amino Acid Uptake Inhibition Assays. The 9L gliosarcoma cells were initially grown as monolayers in T-flasks containing Dulbecco's Modified Eagle's Medium (DMEM) under humidified incubator conditions (37 °C, 5% $\text{CO}_2/95\%$ air). The growth media was supplemented with 10% fetal calf serum and antibiotics (10 000 units/mL penicillin and 10 mg/mL streptomycin). The growth media was replaced three times per week, and the cells were passaged so that the cells would reach confluency in a week's time.

When the monolayers were confluent, cells were prepared for experimentation in the following manner. Growth media was removed from the T-flask, and the monolayer cells were exposed to 1 X trypsin:EDTA for ~1 min to weaken the protein attachments between the cells and the flask. The flask was then slapped, causing the cells to release. Supplemented media was added to inhibit the proteolytic action of the trypsin, and the cells were aspirated through an 18 Ga needle until they were monodisperse. A sample of the cells was counted under a microscope using a hemocytometer, and the live/dead fraction was estimated through trypan blue staining (>98% viability). The remainder of the cells was placed into a centrifuge tube and centrifuged at 75G for 5 min, and the supernatant was removed. The cells were then resuspended in amino acid/serum-free DMEM salts.

In this study, approximately 4.55×10^5 cells were exposed to either [^{18}F]**5a** or [^{18}F]**5b** (5 μCi) in 3 mL of amino acid free media \pm transporter inhibitors (10 mM) for 30 min under incubator conditions in 12 mm × 75 mm glass vials. Each assay condition was performed in duplicate. After incubation, cells were twice centrifuged (75G for 5 min) and rinsed with ice-cold amino acid/serum-free DMEM salts to remove residual activity in the supernatant. The vials were placed in a Packard Cobra II Auto-Gamma counter, the raw counts were decay-corrected, and the activity per cell number was determined. The data from these studies (expressed as percent uptake relative to control) were graphed using Excel, with statistical comparisons between the groups analyzed using a one way ANOVA (GraphPad Prism software package).

Tumor Induction and Animal Preparation. All animal experiments were carried out under humane conditions and were approved by the Institutional Animal Use and Care Committee (IUCAC) at Emory University. Rat 9L gliosarcoma cells were implanted into the brains of male Fischer rats as described previously.¹⁴ Briefly, anesthetized rats placed in a stereotactic head holder were injected with a suspension of 4×10^4 rat 9L gliosarcoma cells (1×10^7 per mL) in a location 3 mm right of midline and 1 mm anterior to the bregma at a depth of 5 mm deep to the outer table. The injection was performed over the course of 2 min, and the needle was withdrawn over the course of 1 min to minimize the backflow of tumor cells. The burr hole and scalp incision were closed, and the animals were returned to their original colony after recovering from the procedure. Intracranial tumors developed that produced weight loss, apathy, and hunched posture in the tumor-bearing rats, and the animals were used at 17–19 days after implantation. Of the 30 animals implanted with tumor cells, 25 developed tumors visible to the naked eye upon dissection and were used in the study.

Rodent Biodistribution Studies. The same procedures were used to evaluate [^{18}F]**5a** and [^{18}F]**5b** separately in rodents. The tissue distribution of radioactivity was deter-

mined in 16 normal male Fischer 344 rats (200–250 g) after intravenous injection of ~85 μCi of [^{18}F]**5a** or [^{18}F]**5b** in 0.3 mL of sterile water. The animals were allowed food and water ad libitum before the experiment. Following anesthesia induced with an intramuscular injection of 0.1 mL/100 g of a 1:1 ketamine (500 mg/mL):xylazine (20 mg/mL) solution, the radiolabeled amino acid was injected into the rats via tail vein catheters. Groups of four rats were killed at 5, 30, 60, and 120 min after injection of the dose. The animals were dissected, and selected tissues were weighed and counted along with dose standards in a Packard Cobra II Auto-Gamma Counter. The raw counts were decay-corrected, and the counts were normalized as the percent of total injected dose per gram of tissue (%ID/g). A comparison of the uptake of activity in the tissues at each time point was analyzed using a one way ANOVA (GraphPad Prism software package).

The tissue distribution of radioactivity was also determined in tumor-bearing Fischer 344 rats following intravenous injection of ~35 μCi of [^{18}F]**5a** or [^{18}F]**5b** in 0.3 mL of sterile water. The procedure was similar to that already described for normal rats with the following modifications. The tail vein injections were performed in awake animals using a RTV-190 rodent restraint device (Bairtree Scientific) to avoid mortality accompanying anesthesia in the presence of an intracranial mass. The animals were killed at 5, 60, or 120 min postinjection. The same tissues were assayed as in normal rats with the addition of the tumor tissue, and the corresponding region of brain contralateral to the tumor was excised and used for comparison. The uptake in the tumor and contralateral brain at each time point was compared via a two-tailed t -test for paired observations (GraphPad Prism software package).

Acknowledgment. We acknowledge the use of Shared Instrumentation provided by grants from the NIH and the NSF for the mass spectroscopy data.

Supporting Information Available: Mass spectroscopy data for compound **12b**. This material is available free of charge via the Internet at <http://pubs.acs.org>.

References

- Buonocore, E. Comparison of PET with conventional imaging techniques. *Clinical Positron Emission Tomography*; Mosby-Year Book, Inc.: St. Louis, MO, 1992; pp 17–22.
- Langleben, D. D.; Segall, G. M. PET in differentiation of recurrent brain tumor from radiation injury. *J. Nucl. Med.* **2000**, *41*, 1861–1867.
- Griffeth, L. K.; Rich, K. M.; Dehdashti, F.; et al. Brain metastases from noncentral nervous system tumors: evaluation with PET. *Radiology* **1993**, *186*, 37–44.
- Conti, P. S. Introduction to imaging brain tumor metabolism with positron emission tomography. *Cancer Invest.* **1995**, *13*, 255–259.
- Kubota, K.; Yamada, S.; Kubota, R.; et al. Intratumoral distribution of fluorine-18-fluorodeoxyglucose in vivo: high accumulation in macrophages and granulation tissue studied with microradiography. *J. Nucl. Med.* **1992**, *33*, 1972–1980.
- Kubota, R.; Kubota, K.; Yamada, S.; et al. Microautoradiographic study for the differentiation of intratumoral macrophages, granulation tissues and cancer cells by the dynamics of fluorine-18-fluorodeoxyglucose uptake. *J. Nucl. Med.* **1993**, *34*, 104–112.
- Ogawa, T.; Shishido, F.; Kanno, I.; et al. Cerebral glioma: evaluation with methionine PET. *Radiology* **1993**, *186*, 45–53.
- Jager, P. L.; Vallburg, W.; Pruijm, J.; et al. Radiolabeled amino acids: basic aspects and clinical applications in oncology. *J. Nucl. Med.* **2001**, *42*, 432–445.
- Derlon, J. M. The in vivo metabolic investigation of brain gliomas with positron emission tomography. *Adv. Technol. Standards Neurosurgery* **1998**, *24*, 41–76.
- Iuchi, T.; Iwadate, Y.; Namba, H.; et al. Glucose and methionine uptake and proliferative activity in meningiomas. *Neurol. Res.* **1999**, *21*, 640–644.
- Conti, P. S.; Sordillo, P. P.; Schmall, B.; et al. Tumor imaging with carbon-11 labeled α -aminoisobutyric acid (AIB) in a patient with advanced malignant melanoma. *Eur. J. Nucl. Med.* **1986**, *12*, 353–356.
- Inoue, T.; Shibasaki, T.; Oriuchi, N.; et al. ^{18}F α -methyl tyrosine PET studies in patients with brain tumors. *J. Nucl. Med.* **1999**, *40*, 399–405.

- (13) Weber, W. A.; Wester, H. J.; Grosu, A. L.; et al. *O*-(2-[¹⁸F]-Fluoroethyl)-L-tyrosine and L-[methyl-¹¹C]methionine uptake in brain tumors: initial results of a comparative study. *Eur. J. Nucl. Med.* **2000**, *27*, 542–549.
- (14) Shoup, T. M.; Olson, J.; Hoffman, J. M.; et al. Synthesis and evaluation of [¹⁸F]1-amino-3-fluorocyclobutane-1-carboxylic acid to image brain tumors. *J. Nucl. Med.* **1999**, *40*, 331–338.
- (15) Palacin, M.; Estévez, R.; Bertran, J.; Zorzano, A. Molecular biology of mammalian plasma membrane amino acid transporters. *Physiol. Rev.* **1998**, *78*, 969–1054.
- (16) Bussolati, O.; Uggeri, J.; Silvana, B.; et al. The stimulation of Na, K, Cl cotransport of system A for neutral amino acid transport is a mechanism for cell volume increase during the cell cycle. *FASEB J.* **1996**, *10*, 920–926.
- (17) Saier, M. H.; Daniels, G. A.; Boerner, O.; Lin, J. Neutral amino acid transport systems in animal cells: potential targets of oncogene action and regulators of cell growth. *J. Membr. Biol.* **1988**, *104*, 1–20.
- (18) Conti, P. S.; Sordillo, E. M.; Sordillo, P. P.; Schmall, B. Tumor localization of α -aminoisobutyric acid (AIB) in human melanoma heterotransplants. *Eur. J. Nucl. Med.* **1985**, *10*, 45–47.
- (19) Uehara, H.; Miyagawa, T.; Tjuvajev, J.; et al. Imaging experimental brain tumors and 1-aminocyclopentane carboxylic acid and α -aminoisobutyric acid: comparison to fluorodeoxyglucose and diethylenetriaminepentaacetic acid in morphologically defined tumor regions. *J. Cereb. Blood Flow Metab.* **1997**, *17*, 1239–1253.
- (20) Fross, R. D.; Warnke, P. C.; Groothuis, D. R. Blood flow and blood-to-tissue transport in 9L gliosarcomas: the role of the brain tumor model in drug delivery research. *J. Neurooncol.* **1991**, *11*, 185–197.
- (21) Dunzendorfer, U.; Schmall, R. E.; Bigler, P. B.; et al. Synthesis and body distribution of α -aminoisobutyric acid-L-¹¹C in normal and prostate cancer-bearing rat after chemotherapy. *Eur. J. Nucl. Med.* **1981**, *6*, 535–538.
- (22) Shotwell, M. A.; Kilberg, M. S.; Oxender, D. L. The regulation of neutral amino acid transport in mammalian cells. *Biochim. Biophys. Acta* **1983**, *737*, 267–284.
- (23) Christensen, H. N.; Oxender, D. L.; Liang, M.; Vatz, K. A. The use of *N*-methylation to direct the route of mediated transport of amino acids. *J. Biol. Chem.* **1965**, *240*, 3609–3616.
- (24) Nägren, K.; Sutinen, E.; Jyrkkö, S. [*N*-methyl-¹¹C]MeAIB, a tracer for system A amino acid transport: preparation form [¹¹C]-methyl triflate and HPLC metabolite analysis of plasma samples after intravenous administration in man. *J. Labelled Compd. Radiopharm.* **2000**, *43*, 1013–1021.
- (25) Thierry, J.; Yue, C.; Potier, P. 2-phenyl isopropyl and *tert*-butyl trichloroacetimidates: useful reagents for ester preparation of *N*-protected amino acids under neutral conditions. *Tetrahedron Lett.* **1998**, *39*, 1557–1560.
- (26) Weiland, D. M.; Kilbourn, M. R.; Yang, D. J.; et al. NMDA receptor channels: Labeling of MK-801 with Iodine-125 and Fluorine-18. *Appl. Radiat. Isot.* **1988**, *39*, 1219–1225.
- (27) Van Dort, M. E.; Jung, Y. W.; Sherman, P. S.; et al. Fluorine for hydroxy substitution in biogenic amines: asymmetric synthesis and biological evaluation of fluorine-18-labeled β -fluorophenyl-alkylamines as model systems. *J. Med. Chem.* **1995**, *38*, 810–815.
- (28) Boulton, L. T.; Stock, T.; Raphy, J.; Horwell, D. C. Generation of unnatural α,α -disubstituted amino acid derivatives from cyclic sulfamidates. *J. Chem. Soc., Perkins Trans. 1* **1999**, 1421–1429.
- (29) Posakony, J. J.; Tewson, T. J. Progress in the synthesis of [¹⁸F]-fluoroamines; precursors to β -selective adrenergic ligands. *J. Labelled Compd. Radiopharm.* **1999**, *42*, S527–S529.
- (30) Hanson, R. W.; Law, H. D. Substituted diphenylmethyl protecting groups in peptide synthesis. *J. Chem. Soc.* **1965**, 7285–7297.
- (31) Goodacre, J.; Ponsford, R. J.; Stirling, I. Selective removal of the *tert*-butyloxycarbonyl protecting group in the presence of *tert*-butyl and *p*-methoxybenzyl esters. *Tetrahedron Lett.* **1975**, *42*, 3609–3612.
- (32) Alexoff, D. L.; Casati, R.; Fowler, J. S.; et al. Ion chromatographic analysis of high specific activity ¹⁸FDG preparations and detection of the chemical impurity 2-deoxy-2-chloro-D-glucose. *Int. J. Rad. Appl. Instrum. Part A* **1992**, *43*, 1313–1322.
- (33) Betz, A. L.; Goldstein, G. W. Polarity of the blood-brain barrier: neutral amino acid transport into isolated brain capillaries. *Science* **1978**, *202*, 225–227.
- (34) Kubota, K.; Yamada, K.; Fukada, H.; et al. Tumor detection with carbon-11-labeled amino acids. *Eur. J. Nucl. Med.* **1984**, *9*, 136–140.
- (35) Boger, D. L.; Palanki, M. S. S. Functional analogues of CC-1065 and the duocarmycins incorporating the 9a-(chloromethyl)-1,2,9,9a-tetrahydrocyclopropa[*c*]benz[*e*]indol-4-one (C2BI) alkylation subunit: synthesis and preliminary DNA alkylation studies. *J. Am. Chem. Soc.* **1992**, *114*, 9318–9327.
- (36) Dutta, A. K.; Xu, C.; Reith, M. E. A. Structure–activity relationship studies of novel 4-[2-[bis(4-fluorophenyl)methoxy]ethyl]-1-(3-phenylpropyl)piperidine analogues: synthesis and biological evaluation at the dopamine and serotonin transporter sites. *J. Med. Chem.* **1996**, *39*, 749–756.

JM010241X